Intrinsic localized spin-wave resonances in ferromagnetic chains with nearest- and next-nearest-neighbor exchange interactions

R. Lai, S. A. Kiselev,* and A. J. Sievers
Laboratory of Atomic and Solid State Physics and Materials Science Center, Cornell University, Ithaca, New York 14853-2501
(Received 28 April 1997)

We demonstrate analytically and numerically that the simplest isotropic ferromagnetic one-dimensional system to show intrinsic localized spin-wave resonances requires only isotropic exchange interactions between first and second neighbors. Our numerical simulations indicate that the lifetime of these intrinsic localized spin-wave resonances depends on the mode parity, the maximum spin deviation, and the relative strength of the next-nearest-neighbor–to–nearest-neighbor exchange interactions. In the small amplitude limit translating localized spin-wave resonances behave like solitons but for larger amplitudes they are scattered by the discreteness of the lattice and decay by radiating plane spin-wave modes. [S0163-1829(97)05134-5]

I. INTRODUCTION

A wide variety of translationally invariant, nonlinear physical systems can support long-lived, spatially localized excitations under certain conditions. These nonlinear localized excitations are usually modeled as solitons, which are solutions of completely *integrable* nonlinear wave equations and have infinite lifetimes.[1,2] In particular, solitary excitations in one-dimensional magnetic systems have been extensively investigated in the continuum limit.[3] The situation for discrete systems is quite different since few discrete lattices are integrable, except for the Toda lattice[4] and the Ablowitz-Ladik lattice[5] and these lattice models appear to be integrable by construction rather than motivated by realistic physical systems. Since the discovery of intrinsic localized modes (ILM's) in perfectly periodic but anharmonic nonintegrable discrete lattices,[6–9] attention has focused on the study of localization in various periodic lattices where both *nonlinearity* and *discreteness* play important roles and the study of this *intrinsic localization* in various nonlinear periodic lattices is proving quite general.[10–18] In magnetic systems, it has been shown that intrinsic localized spin wave modes (ILSM's) can also occur in perfect but nonintegrable magnetic chains.[19–23] In the presence of a strong magnetic field perpendicular to the easy plane, both even-parity and odd-parity ILSM's appear in easy-plane Heisenberg ferromagnetic chains when the strength of single-ion anisotropy exceeds a certain value[20,21] so that the ILSM frequencies are above the linear spin-wave band. In antiferromagnetic chains intrinsic localized spin-wave gap modes (ILSG's) have been shown to exist within the gap produced by either exchange anisotropy or single-ion anisotropy.[19,22] Like their vibrational counterpart, these highly localized ILSM's involve only a few sites and have amplitude-dependent frequencies outside the harmonic plane-wave bands. More recently, it has been demonstrated numerically that in-band nonlinear localized excitations in easy-plane antiferromagnetic chains can occur and that they are long lived,[23] although from analytical work lattice dynamics resonant modes already have been proposed to be a natural consequence of intrinsic localization.[24] The key feature of the dynamics of an in-band intrinsic localized spin-wave resonance (ILSR) is the uncoupling of an opticlike ILSR from the acoustic linear spin-wave spectrum. So far the intrinsic localization of spin waves has been identified with the anisotropy contribution in the magnetic properties of chains with nearest-neighbor interactions.

Here we demonstrate that intrinsic localization can occur in *isotropic* chains of classical spins coupled ferromagnetically through both nearest-neighbor (NN) and next-nearest-neighbor (NNN) exchange interactions. We find that long-lived ILSR's can exist near the Brillouin zone boundary when the strength of NNN interaction relative to the NN interaction exceeds a threshold. The dynamic properties and mobility of the resulting ILSR's are investigated in some detail.

In the next section the stationary intrinsic spin-wave resonances are derived. Both odd-parity and even-parity modes are found that the dependence of these eigenfrequencies on the maximum spin deviation is determined, then molecular-dynamics simulations are used to estimate the lifetimes of these modes. In Sec. III stability analysis of extended plane-wave modes is used to predict under what conditions nonlinear localized modes will occur. Contact is also made here with envelope solitons associated with the continuum approximation. Finally, the translational properties of these excitations are examined in Sec. IV. Both motion of a single ILSR and collisions between ILSR's are considered. The conclusions follow.

II. STATIONARY INTRINSIC LOCALIZED SPIN-WAVE RESONANCES

A. The 1D model

Previous study has shown that no intrinsic localization occurs in isotropic ferromagnetic chain with nearest-neighbor interactions.[20] Here we consider a one-dimensional ferromagnetic chain of N spins which are coupled through both nearest-neighbor (NN) and next-nearest-neighbor (NNN) isotropic exchange interactions. Hence, the Hamiltonian to be examined is

$$H = -2J_1 \sum_n \mathbf{S}_n \cdot \mathbf{S}_{n+1} - 2J_2 \sum_n \mathbf{S}_n \cdot \mathbf{S}_{n+2}, \qquad (1)$$

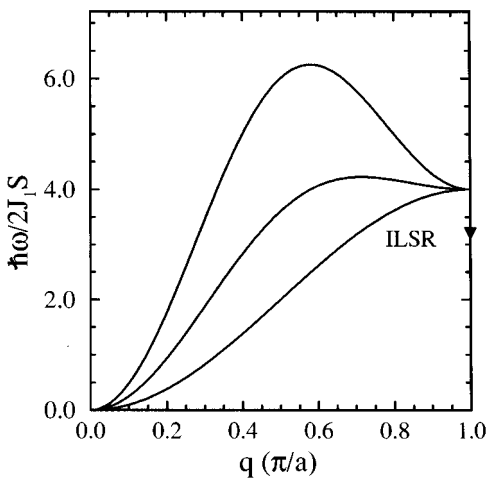

FIG. 1. Dispersion curves of linear spin waves in isotropic ferromagnetic chains with both nearest-neighbor (NN) and next-nearest-neighbor (NNN) exchange interactions. From top to bottom, the relative strength of the NNN coupling $A=J_2/J_1$ are 1.0, 0.4, and 0, respectively. When A is greater than 1/4 the maximum frequency would appear at $q_{\max}$ rather than the Brillouin-zone boundary. The ILSR arrow identifies the frequency of the intrinsic localized spin-wave resonance described in the text.

where both the NN coupling constant J_1 and the NNN coupling constant J_2 are positive, and periodic boundary conditions are to be applied.

Since the chain is isotropic we assume that all spins align along the z axis in the ground state without losing generality. To investigate spin deviations from the ground state we define $s_n^{\pm}=(S_n^x \pm iS_n^y)/S$, and $s_n^z=S_n^z/S$ in the usual way where S is the magnitude of spins. In these circular coordinates, the equations of motion are given by

$$i\frac{\hbar}{2J_1S}\frac{ds_n^+}{dt}=s_n^+(s_{n-1}^z+s_{n+1}^z+As_{n-2}^z+As_{n+2}^z) - s_n^z(s_{n-1}^+ + s_{n+1}^+ + As_{n-2}^+ + As_{n+2}^+), \quad (2)$$

where the dimensionless parameter $A=J_2/J_1$ measures the strength of NNN coupling relative to NN coupling. Hereafter, we treat the spins as classical vectors. Since $s_n^z=\sqrt{1-|s_n^+|^2}$, Eq. (2) is intrinsically nonlinear in s_n^+. The linear spin-wave dispersion curve can be obtained by linearizing Eq. (2), i.e., approximating s_n^z by one. Introducing $s_n^+=s_0e^{i(qna-\omega t)}$ the dispersion curve becomes

$$\omega(q)=\frac{8J_1S}{\hbar}\left[\sin^2\left(\frac{qa}{2}\right)+A\,\sin^2(qa)\right], \quad (3)$$

where $q=(2\pi/Na)n$, $(n=0,\pm1,...,\pm N/2)$, and a is the lattice spacing between adjacent spins.

Figure 1 shows the dispersion curves for different NNN coupling strengths. The frequency of the Brillouin-zone boundary mode is independent of the NNN coupling because a precessing spin is in phase with its NNN's in this mode. However, the NNN coupling tends to raise the dispersion curve at intermediate wave numbers so that its maximum frequency $\omega_{\max}$ may appear at a wave number $q_{\max}$ other than π/a, i.e.,

$$q_{\max}=\frac{\pi}{a}-\frac{1}{a}\cos^{-1}\left(\frac{1}{4A}\right) \quad \text{and}$$

$$\omega_{\max}=\frac{2J_1}{\hbar}(1+4A)\left(1+\frac{1}{4A}\right), \quad (4)$$

when A is greater than 1/4. It may appear that intrinsic localization could first occur at $q_{\max}$ with frequency above $\omega_{\max}$; however, the nonlinear terms in Eq. (2) tend to lower the frequency, and indeed, no intrinsic localized modes are found at $q_{\max}$. The fact that the dispersion curve can have its maximum frequency at a wave number other than the Brillouin-zone boundary opens up a new possibility that ILSR's may occur at the band edge. We will show later that the critical value of $A(=1/4)$ is closely related to the existence of ILSR's in this lattice.

B. ILSR's at the zone boundary

To find the eigenvector of a stationary ILSR below the Brillouin-zone boundary value all nonlinear terms must be included. Inserting the ansatz

$$s_n^+=s_ne^{-i\omega_r t},\quad s_n^*=s_n,\qquad \text{and}\quad s_n^z=(1-s_n^2)^{1/2} \quad (5)$$

into Eq. (2) gives the time-independent equation

$$\frac{\hbar\omega_r}{2J_1S}s_n=s_n[\sqrt{1-s_{n-1}^2}+\sqrt{1-s_{n+1}^2}+A(\sqrt{1-s_{n-2}^2}+\sqrt{1-s_{n+2}^2})]-\sqrt{1-s_n^2} \times[s_{n-1}+s_{n+1}+A(s_{n-2}+s_{n+2})], \quad (6)$$

where ω_r is the frequency of the ILSR. Given the maximum spin deviation at the mode center $s_{\max}$, Eq. (6) can be solved numerically by using the globally convergent Newton method[25] to obtain the eigenvector shape and the frequency of the ILSR. The eigenvectors can be classified in terms of their parities. Both an odd-parity mode and an even-parity mode an occur for a range of parameter A.

C. Eigenvector shapes

As an illustration, the eigenvectors of an odd-parity ILSR and an even-parity ILSR for the set of parameters $A=1.0$ and $s_{\max}=0.7$ are plotted in Figs. 2(a) and 2(b), respectively. The one-dimensional chain consists of 256 spins with periodic boundary condition. The symmetry center of the odd-parity mode is on the lattice site with maximum spin deviation, while the symmetry center of the even-parity mode is in the middle between two adjacent sites with maximum spin deviation. The common feature of both ILSR's is that the spin deviations do not disappear with increasing distance from the center. Instead the localized excitations evolve into a weak plane wave pattern, as expected for a resonance.[23] Although breathers with extended plane-wave tails of nondecaying amplitude were found before both in the continuous ϕ^4 model[26] and in discrete nonlinear lattices with substrate potentials,[27] the ILSR's in magnetic chains are fundamentally different from these. In previously found resonant breathers, the localized center oscillates at a fundamental frequency *outside* the liner spectrum while the extended plane-

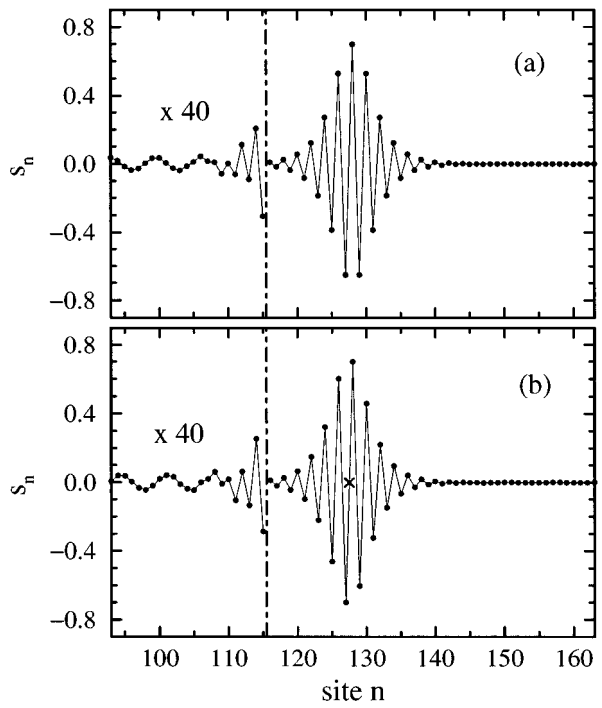

FIG. 2. Shapes of stationary intrinsic localized spin-wave resonances of different parities. The ferromagnetic chain contains 256 spins with the parameter $A=1.0$. Both modes have the same maximum spin deviation $s_{max}=0.7$. (a) Odd-parity mode, the symmetry center is on the lattice site $n=128$. The left side shows a factor 40 expansion of the ordinate to display the plane-wave character in the wings. (b) Even-parity mode, the symmetry center (the X) is between two adjacent sites. The left side shows the same factor 40 expansion and a sign alternation to illustrate the resonant mode plane-wave character.

wave tail oscillates at the higher harmonics of the fundamental frequency. The extended plane-wave exists in those resonant breathers because the nonlinear terms in the equation of motion generate high harmonics that are in the linear spectrum. However, the fundamental frequency of the ILSR's found here in these magnetic chains is in the linear spectrum, and the ILSR's are monochromatic.

The wave numbers associated with the weak plane wave pattern can be identified from the Fourier transformation

$$|s(q)|^2=\left|\sum_n s_n\exp(iqna)\right|^2. \tag{7}$$

In addition to Fourier components centered at $q=\pi/a$, there is a sharp peak located at q_l with a strength that grows with increasing maximum spin deviation. As expected, substituting q_l into the linear spin dispersion relation Eq. (3) yields the corresponding resonance frequency ω_r.

For a given maximum spin deviation both the odd-parity mode and the even-parity mode become more localized and the amplitude of the off-center plane wave component increases with decreasing relative strength of the NNN interaction, while when the strength of the NNN interaction is fixed the eigenvector shape of an ILSR becomes more localized and the amplitude of off-center plane-wave component increases with increasing maximum spin deviation at the center. Our numerical search did not find localized solution when A is less than 1/4. Here the value of 1/4 is only an estimate, which will be accurately determined later from both the stability analysis of extended band edge mode and a continuum approximation study. As A approaches 1/4 from above, the linear spin-wave dispersion curve becomes flat near $q=\pi/a$ and hence has a high density of states at the Brillouin zone boundary. The localized center strongly interacts with the linear spectrum so that the amplitude of plane-wave tail increases rapidly with the maximum spin deviation at the center. The amplitude of the plane-wave tail could be comparable to that of the center when the latter is beyond a certain value for a chain with A close to 1/4. However, the larger the parameter A, the smaller the amplitude of plane-wave tail for a given maximum spin deviation at the center. For example, $|s_{tail}/s_{max}|$ is still less than 0.01 when s_{max} is as large as 0.85 in a chain with $A=1.0$.

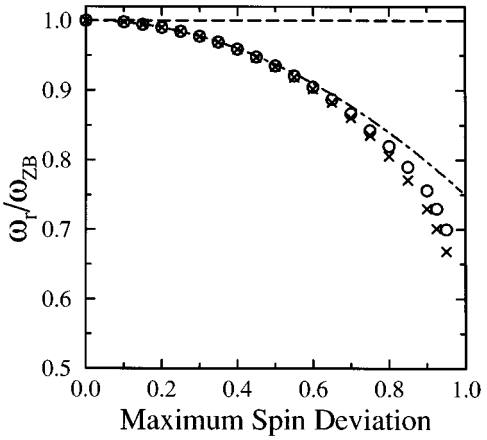

FIG. 3. Dependence of the frequency of stationary ILSR on its maximum spin deviation. The ferromagnetic chain contains 256 spins with the parameter $A=1.0$. Open circles are the frequencies of odd-parity ILSR's, and crosses are the frequencies of even-parity ILSR's. The dot-dashed line is the continuum approximation given by Eq. (20c). ω_{ZB} is the frequency of linear spin wave at the Brillouin boundary.

D. Dependence of the mode frequency on the maximum spin deviation

Figure 3 shows the dependence of the frequency of the ILSR on its maximum spin deviation in a ferromagnetic chain of 256 spins. The NNN interaction parameter A is 1.0. The open circles and crosses denote the frequencies of the odd-parity ILSR's and the frequencies of the even-parity ILSR's, respectively. The frequencies are found by numerically solving Eq. (6) with periodic boundary condition. For small spin deviations, the frequency of an ILSR lies close to the Brillouin-zone boundary frequency of the linear-spin-wave band. With increasing spin deviation the mode becomes more localized and its frequency drops further into the linear spin-wave band. For fixed maximum spin deviation, the frequency of the even-parity ILSR is lower than that of the odd-parity ILSR. Although there is no apparent distinction between odd-parity modes and even-parity modes with small maximum spin deviations (and indeed they are expected to approach the same continuum limit as $s_{max}\rightarrow 0$) the

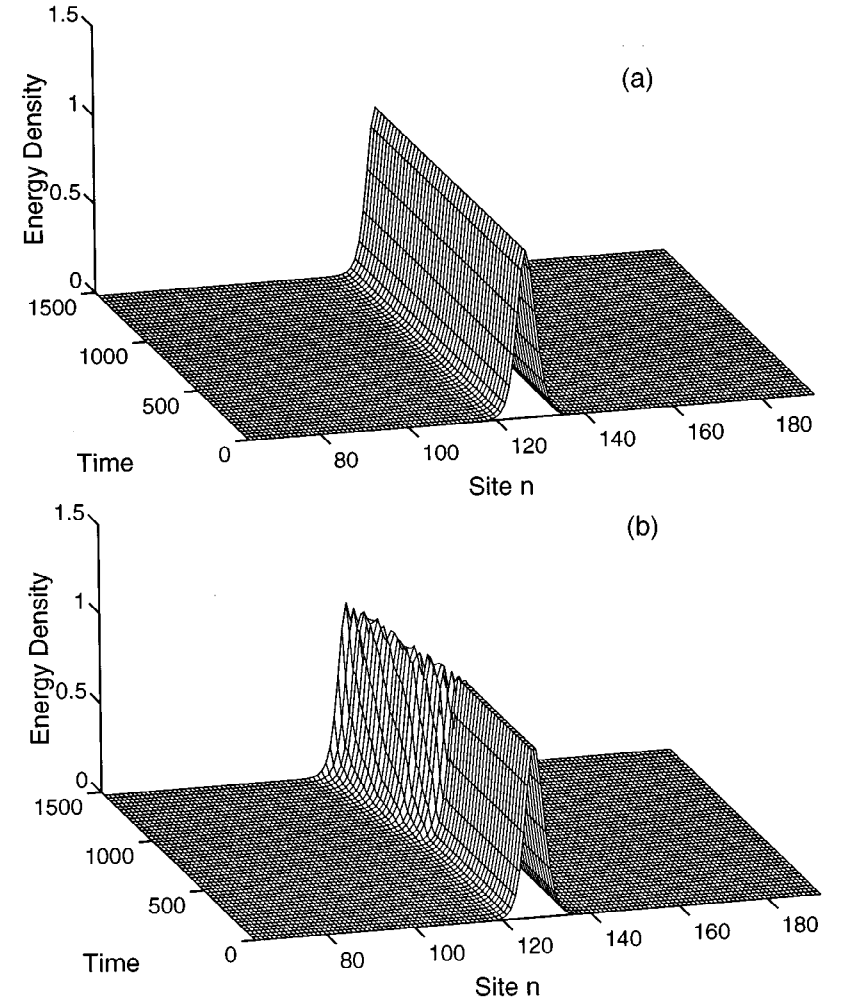

FIG. 4. Time evolution of the energy density distributions of the ILSR's shown in Figs. 2(a) and 2(b). The energy density shown here is measured from the ground-state energy density and is in units of $2J_1$. Time is measured in units of T_{ZB}. (a) Odd-parity ILSR. (b) Even-parity ILSR.

difference between them increases as s_{max} increases. The dot-dashed line is the continuum approximation frequency obtained later in Sec. III B, which is in good agreement with the discrete results up to $s_{max}=0.5$.

E. Lifetime of ILSR's

Since the localized excitation is in resonance with the plane-wave spectrum it is expected that an ILSR becomes unstable and delocalizes after sufficient time. With the eigenvectors obtained by numerically solving Eq. (6) providing the initial conditions, the lifetime of ILSR's can be investigated by means of molecular-dynamics (MD) simulations. In MD simulations the discrete equations of motion for the xyz spin components are integrated numerically by using the fourth-order Runge-Kutta method with a time step of $T_{ZB}/200$ where T_{ZB} is the period of the linear spin-wave mode at the Brillouin zone boundary and $T_{ZB}=\pi\hbar/4J_1S$. At each step conservation of energy and spin length (to 1 part in 10^5) serve as checks on the numerical accuracy. The numerical simulations demonstrate that the lifetime of an ILSR depends on three factors: (1) its parity, (2) the maximum spin deviation, and (3) the relative strength of the NNN interaction A.

At sufficient small amplitudes, ILSR's of both parities can last many hundreds of periods. With increasing amplitude the emission of plane-waves from the ILSR's is observed and the larger the amplitude the faster the decay, however we find that the even-parity mode is more unstable than the odd-parity mode. Figures 4(a) and 4(b) show the time evolution of the energy density given by

$$e(n)=-J_1\mathbf{s}_n\cdot(\mathbf{s}_{n-1}+\mathbf{s}_{n+1})-J_2\mathbf{s}_n\cdot(\mathbf{s}_{n-2}+\mathbf{s}_{n+2}) \quad (8)$$

for an odd-parity ILSR and an even-parity ILSR with modest spin deviation ($s_{max}=0.7$), respectively. The energy density is measured from the ground-state value. The chain under consideration contains 256 spins with periodic boundary condition. The odd-parity mode preserves its initial shape over the entire period of $1500T_{ZB}$. The figure shows that the even-parity mode starts to move and decay while remains localized after about $750T_{ZB}$.

The decay of an ILSR is due to its coupling to the linear spin-wave spectrum. As the strength of the NNN interaction increases, the wave number of the spin wave that is in resonance with the localized excitation moves away from the band edge so that the coupling between the ILSR to the spin wave becomes weaker and hence its lifetime increases.

III. EXISTENCE CONDITION FOR ILSR's

Our numerical calculations indicate that the existence of ILSR's depends strongly on the relative strength of the NNN

interaction. The interrelation between the modulational instability of the extended band edge plane waves and the existence of spatially localized excitations has been established in a number of nonlinear lattices.[28–34] Hence the stability analysis of an extended plane wave provides a useful way to predict under what conditions nonlinear localized excitation can occur. In this section, the existence condition of ILSR's will be obtained from both linear stability analysis of the extended nonlinear zone-boundary mode and the continuum approximation.

A. Modulational instability of extended nonlinear spin-wave modes

The linear dispersion curve given by Eq. (3) is obtained for spin-wave modes of virtually zero-spin deviation. For finite spin deviation, Eq. (2) has also time-periodic solutions of spatially extended nonlinear spin-wave modes, $s_n^+(t)=s_0 e^{i(qna-\omega t)}$, whose frequency can be obtained as

$$\omega(q)=\frac{8J_1S}{\hbar}\left[\sin^2\left(\frac{qa}{2}\right)+A\,\sin^2(qa)\right](1-s_0^2)^{1/2}, \quad (9)$$

where the deviation s_0 is not negligible, and the nonlinear terms tends to decrease the frequency. The extended spin-wave modes are modulationally unstable under certain conditions.

To determine the parameter space in which they are unstable, we carry out linear stability analysis. Assuming an extended nonlinear spin-wave mode $s_n^+(t)=s_0 e^{i(qna-\omega t)}$ is perturbed so that

$$s_n^+(t)\rightarrow s_n^+(t)=(s_0+b_n+i\psi_n)e^{i(qna-\omega t)}, \quad (10)$$

where the frequency ω is given by Eq. (9) and the perturbations b_n and ψ_n are real and much smaller than s_0 in magnitude. Substituting Eq. (10) into Eq. (2) and keeping only terms linear in b_n and ψ_n, we obtain two linear differential equations for b_n and ψ_n:

$$\frac{\hbar}{2J_1S}\frac{db_n}{dt}=\sqrt{1-s_0^2}\left\{2\begin{pmatrix}\cos qa+\\ A\,\cos 2qa\end{pmatrix}\psi_n-\begin{bmatrix}(b_{n+1}-b_{n-1}\sin qa+\\ (\psi_{n+1}+\psi_{n-1})\cos qa\end{bmatrix}-A\begin{bmatrix}(b_{n+2}-b_{n-2})\sin 2qa+\\ (\psi_{n+2}+\psi_{n-2})\cos 2qa\end{bmatrix}\right\} \quad (11a)$$

and

$$\frac{\hbar}{2J_1S}\frac{d\psi_n}{dt}=-\sqrt{1-s_0^2}\left\{\begin{array}{l}2(\cos qa+A\,\cos 2qa)b_n-\dfrac{s_0^2}{(1-s_0^2)}\begin{bmatrix}(b_{n+1}+b_{n-1}-2b_n\cos qa)+\\ A(b_{n+2}+b_{n-2}-2b_n\cos 2qa)\end{bmatrix}\\ -\begin{bmatrix}(b_{n+1}+b_{n-1})\cos qa-\\ (\psi_{n+1}-\psi_{n-1})\sin qa\end{bmatrix}-A\begin{bmatrix}(b_{n+1}+b_{n-2})\cos 2qa-\\ (\psi_{n+2}-\psi_{n-2})\sin 2qa\end{bmatrix}\end{array}\right\}. \quad (11b)$$

For a chain of N spins, we obtain $2N$ coupled linear differential equations. If the perturbation grows exponentially the extended nonlinear spin wave is modulationally unstable, otherwise it is stable. To obtain the eigenvalues of Eqs. (11a) and (11b), we assume

$$b_n=be^{i(Qna-\Omega_m t)}+\text{c.c.}, \quad (12a)$$

and

$$\psi_n=\psi e^{i(Qna-\Omega_m t)}+\text{c.c.}, \quad (12b)$$

where Q and Ω_m are the wave number and frequency of the modulation wave, respectively. Substituting Eqs. (12a) and (12b) into Eqs. (11a) and (11b), we obtain two coupled linear equations

$$\begin{pmatrix}M_{11} & M_{12}\\ M_{21} & M_{22}\end{pmatrix}\begin{pmatrix}b\\ \psi\end{pmatrix}=0, \quad (13)$$

where the matrix elements of M are given by

$$M_{11}=M_{22}=\frac{\hbar\Omega_m}{2J_1S}-2\sqrt{1-s_0^2}(\sin Qa\,\sin qa+A\,\sin 2Qa\,\sin 2qa), \quad (14a)$$

$$M_{12}=-i2\sqrt{1-s_0^2}[(1-\cos Qa)\cos qa+A(1-\cos 2Qa)\cos 2qa], \quad (14b)$$

and

$$M_{21}=-M_{12}-i\frac{2s_0^2}{\sqrt{1-s_0^2}}[(\cos Qa-\cos qq)+A(\cos 2Qa-\cos 2qa)]. \quad (14c)$$

The dispersion curve of the modulation wave, $\Omega_m(q,Q)$, is determined by the condition that the determinant of the matrix M is zero so that Eq. (13) has nontrivial solutions.

Since the ILSR mode, if it exists, should bifurcate from the band-edge mode, we will focus on the band-edge spin wave. Setting $qa=\pi$, we obtain from the $\det(M)=0$ that

$$\left(\frac{\hbar\Omega_m}{2J_1S}\right)^2=16\sin^2\frac{Qa}{2}\left(1-4A\,\cos^2\frac{Qa}{2}\right)\left\{4A\,\sin^4\frac{Qa}{2}+\left(1-4A-2s_0^2\right)\sin^2\frac{Qa}{2}+s_0^2\right\}. \quad (15)$$

Since the right-hand side (RHS) of Eq. (15) is always positive for $A \leqslant A_c$ with $A_c = 0.25$ regardless of the spin derivation s_0, the extended nonlinear band-edge mode is stable for this parameter range. However, as the relative strength of NNN coupling gets stronger so that $A > A_c$, the extended band-edge mode becomes modulationally unstable to long-wavelength perturbations when the spin deviation exceeds the threshold

$$s_c \approx (4A-1)^{1/2}\frac{\pi}{N}. \tag{16}$$

Here we have made use of the fact that $N \gg 1$ so that $\sin(\pi/N) \approx \pi/N$. In a real system s_c is essentially zero since N is of the order of 10^8. This instability region is also the region in which ILSR's can occur. The critical value of A_c is in agreement with the numerical finding in the previous section.

Figure 5 shows snapshots of the energy density distribution at different times as determined by MD simulation for randomly perturbed extended nonlinear band-edge spin-wave mode in two chains each containing 256 spins with periodic boundary condition. The dot-dashed lines represent the energy density distribution of the ground state. In Figs. 5(a), the relative strength of the NNN interaction $A = 0.2$ is below the critical value of A_c while in Fig. 5(b), $A = 0.6$, above the critical value. The initial spin deviations are the same for both chains, and are given by $s_n = (-1)^n 0.1 + \delta s_n$ where the magnitude of random perturbation $|\delta s_n|$ is less than 0.005. The behavior of the extended band-edge mode is qualitatively different. In a chain with A less than A_c, the energy density distribution remains spatially extended throughout the simulation period, as shown in Fig. 5(a). However, Fig. 5(b) demonstrates that the band edge spin wave is unstable in a chain with A greater than A_c. As a consequence of the modulational instability the extended nonlinear band-edge mode is unstable and evolves into temporal ILSR-like localized excitations. At $t = 360 T_{\mathrm{ZB}}$, the initially uniformly distributed energy has been concentrated into 5 ILSR-like excitations. These ILSR-like excitations move around and gradually decay back into plane waves. This MD simulation demonstrates that the modulational instability of the extended band-edge mode is a possible mechanism for the creation of ILSR excitations from extended modes. Recently, it has been reported that in computer simulations the intrinsic localized vibrational modes in perfect anharmonic lattices with realistic interatomic potentials can be created through the modulational instability by exciting nonlinear extended modes using an optical control scheme.[35]

B. Continuum approximation: Envelope solitons

When the maximum spin deviation of an ILSR is small, it extends over a large number of lattice sites. In this case the magnitude of the spin deviation s_n varies slowly with site index n, and the continuum approximation can be invoked. The continuum approximation can determine the existence condition of ILSR's and provide some properties of small amplitude ILSR's which are expected to be qualitatively correct even for ILSR's in the discrete limit. Since the spatial symmetry of a small-amplitude ILSR is close to that of the corresponding plane wave, we introduce the staggered variable

$$\phi_n = (-1)^n s_n^+, \tag{17}$$

where ϕ_n is complex. Here we do not limit the analysis to the stationary modes but instead assume that the wave number associated with the ILSR is close to the band edge so that both the phase and the magnitude of ϕ_n vary slowly in space. Substituting Eq. (17) into Eq. (2) and neglecting nonlinear terms higher than cubic terms, we obtain, in the continuum approximation, a nonlinear Schrödinger (NLS) type equation for $\phi(x,t)$, namely,

$$i\frac{\partial \phi}{\partial t} = \frac{2J_1 S(1-4A)a^2}{\hbar}\frac{\partial^2 \phi}{\partial x^2} + \frac{8J_1 S}{\hbar}\phi - \frac{4J_1 S}{\hbar}|\phi|^2\phi, \tag{18}$$

where the linear term on the RHS can be eliminated by a simple gauge transformation. The NLS is integrable, and the condition for Eq. (18) to have a localized solution (one-soliton solution) is that the coefficient of the second-order spatial derivative and the coefficient of the cubic nonlinear term be of the same sign, that is, $A > 0.25$. This critical value of A agrees with A_c that we found from the linear stability analysis of the extended nonlinear band edge spin wave.

Equation (18) has both stationary and moving localized solutions when $A > A_c$, which are given by

$$\phi(x,t) = \phi_m \ \mathrm{sech}\left(\frac{x-\nu_e t}{l_e}\right) e^{-i(Kx-\omega_r t+\alpha_0)}, \tag{19}$$

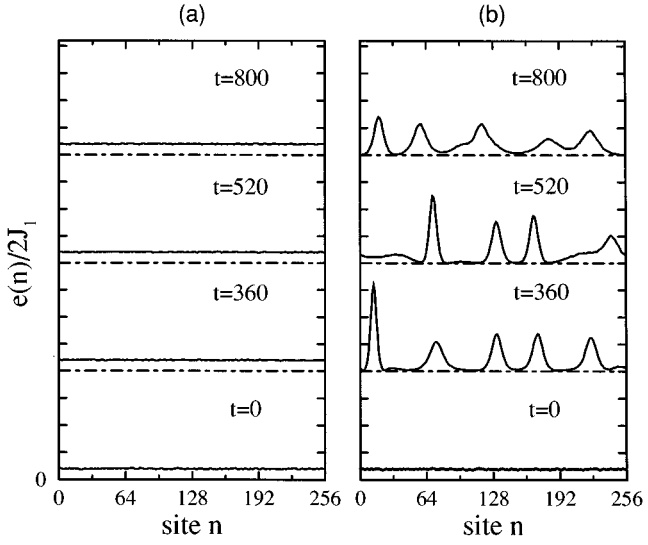

FIG. 5. Modulational instability of extended band-edge spin waves. The snapshots of energy density distributions are determined by MD simulations for randomly perturbed extended band-edge spin waves in chains containing 256 spins with periodic boundary condition. One ordinate unit is 0.05. The dot-dashed lines are the energy density distribution of the ground states. (a) The NNN interaction parameter $A = 0.2$ is less than the critical value A_c. (b) The NNN interaction parameter $A = 0.6$ is greater than the critical value A_c.

where $\pi/a-K$ is the wave number of the carrier wave associated with the ILSR, ϕ_m the maximum spin deviation and α_0 a constant phase factor. The envelope velocity ν_e, the envelope width l_e, and the frequency of the traveling ILSR ω_r are given by

$$\nu_e=-\frac{4J_1Sa^2}{\hbar}(4A-1)K, \tag{20a}$$

$$l_e=\frac{(4A-1)^{1/2}}{\phi_m}a, \tag{20b}$$

and

$$\omega_r=\frac{8J_1S}{\hbar}+\frac{2J_1S(4A-1)}{\hbar}(Ka)^2-\frac{2J_1S}{\hbar}\phi_m^2. \tag{20c}$$

From Eq. (20a), a stationary mode can be obtained by setting $K=0$. The traveling velocity ν_e of the envelope is just the group velocity of the corresponding linear spin wave. From the linear spectrum, Eq. (3), we obtain the group velocity

$$\nu_g=\frac{d\omega}{dq}=\frac{4J_1Sa}{\hbar}(\sin qa+2A\ \sin 2qa) \tag{21}$$

for the linear spin wave with wave number q. Equation (20a) can be recovered by substituting $qa=\pi-Ka(Ka\ll 1)$ into Eq. (21).

Some insight can be gained from Eqs. (20b) and (20c). In the continuum approximation for a given maximum spin deviation, the traveling ILSR and stationary ILSR have the same envelope shape whose width is inversely proportional to the maximum spin deviation and increases with the NNN coupling strength increasing as one might expect. The first term on the right-hand side of Eq. (20c) is just the frequency of the linear band-edge spin wave, and the third term is the anharmonic frequency shift. Since the frequency shift is negative, ω_r, is in the linear spin-wave band. The independence of the mode frequency on the strength of NNN coupling is consistent with the factor that at the Brillouin-zone boundary the spins precess in phase with their NNN's. In the discrete limit where the ILSR is highly localized so that the continuum approximation breaks down, these observations are still expected to be qualitatively correct.

Although the continuum approximation describes well the shape of the center of an ILSR when the maximum spin deviation is small and gives the correct threshold of A, the essential feature of an ILSR, that is, the nondecaying plane-wave tail, does not appear in the solution. The linear dispersion curve of the continuum model described by Eq. (18) can be obtained by setting $\phi_m=0$ in Eq. (20c), which has a parabolic shape with a gap at $K=0$. Hence, the solution Eq. (19) is simply a gap soliton in the continuum model.

IV. TRAVELING ILSR's

So far the large-amplitude localized ILSR excitation is assumed to be described by an elementary excitation with a circular precession frequency ω_r. If an ILSR is traveling through the chain then the circular precession is treated as an internal degree of freedom and the translational motion as an external one. The separation of degrees of freedom is a good approximation only when the wave number of the carrier wave is close to Brillouin zone boundary and hence the traveling velocity of the ILSR is small compared to the phase velocity of the carrier wave. To excite traveling ILSR's we seek solutions of the form

$$\begin{aligned}s_n^{(+)}(t)&=s_n(t)e^{i(qna-\omega_r t)}\\&=(-1)^n\phi_n(t)e^{-i(Kna+\omega_r t)},\end{aligned} \tag{22}$$

where $\phi_n(t)$ is real and

$$qa=\pi-Ka \quad \text{and} \quad Ka\ll 1. \tag{23}$$

Then substituting Eq. (22) into Eq. (2) gives

$$\begin{aligned}\frac{\hbar}{2J_1S}\frac{d\phi_n}{dt}=\sqrt{1-\phi_n^2}[&(\phi_{n-1}-\phi_{n+1})\sin Ka\\&-A(\phi_{n-2}-\phi_{n+2})\sin 2Ka]\end{aligned} \tag{24a}$$

and

$$\begin{aligned}\frac{\hbar\omega_r}{2J_1S}\phi_n=\phi_n&\sqrt{1-\phi_{n-1}^2}+\sqrt{1-\phi_{n+1}^2}+A\sqrt{1-\phi_{n-2}^2}\\&+\sqrt{1-\phi_{n+2}^2}+\sqrt{1-\phi_n^2}[(\phi_{n-1}+\phi_{n+1})\cos Ka\\&-A(\phi_{n-2}+\phi_{n+2})\cos 2Ka].\end{aligned} \tag{24b}$$

Equation (24a) determines the traveling velocity of the ILSR. As expected a stationary ILSR would be found if we set $Ka=0$ in Eq. (24a). Equation (24b) determines the envelope of the traveling ILSR and can be transformed back to Eq. (6) for $Ka=0$.

A. Single traveling ILSR

In the discrete limit (large spin deviation), the envelope of a traveling ILSR can be found by numerically solving Eq. (24b). When the maximum spin deviation of a traveling ILSR is small so that it extends over a large number of lattice sites the continuum approximation can be invoked to simplify the problem. The traveling envelope soliton solutions are given by Eq. (19). Once the initial envelope shape of an ILSR is obtained the MD simulations can be used to investigate its motion. The chain under consideration contains 256 spins and the periodic boundary condition is applied in all MD simulations in this section.

Figure 6(a) shows the time evolution of an ILSR with $s_{\max}=0.3$, $Ka=\pi/32$, and $A=1.0$. Since the maximum spin deviation is small, the initial envelope shape can be obtained from the continuum approximation, Eq. (19). In this case the characteristic off-central plane-wave pattern of a resonant mode, which would occur if Eq. (24b) is solved, is negligible. It appears that this small-amplitude ILSR can travel freely through the lattice with the velocity given by Eq. (20a), and no apparent decay or slow down is observed. As the maximum spin deviation increases the continuum ap-

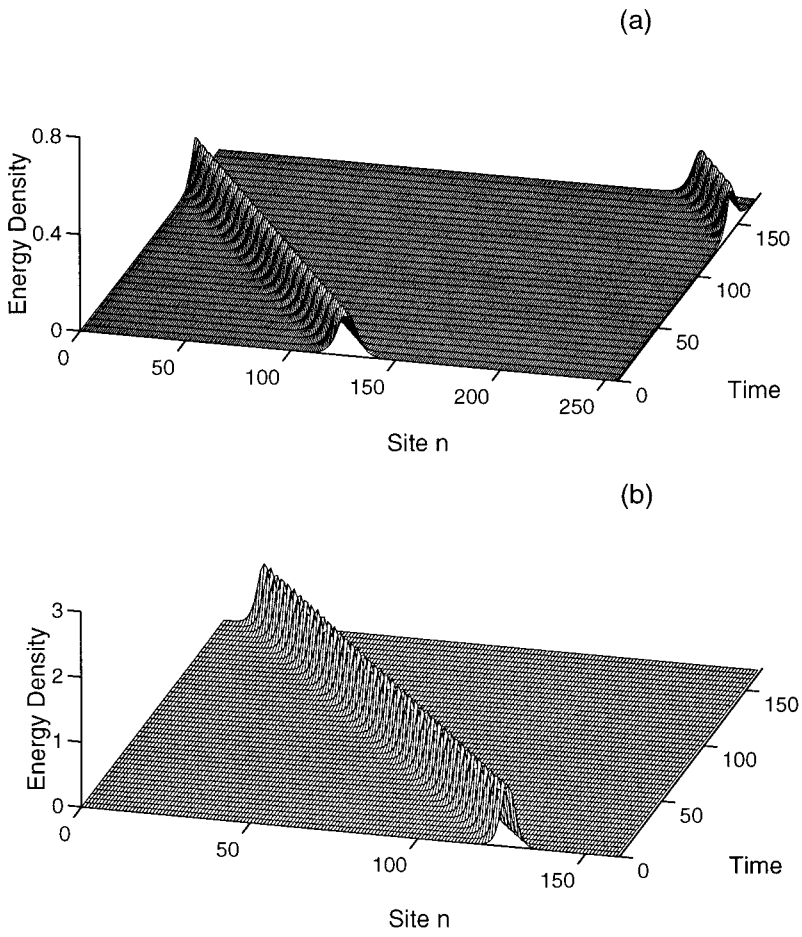

FIG. 6. Time evolution of the energy density distribution of two traveling ILSR's with different sets of parameters. (a) $A=1.0$, $s_{\max}=0.3$, and $Ka=\pi/32$. (b) $A=1.0$, $s_{\max}=0.7$, and $Ka=\pi/32$. Each chain contains 256 spins. For clarity, only part of the chain is shown in (b). The energy density shown here is measured from the ground-state energy density and is units of $2J_1$. Time is measured in units of T_{ZB}.

proximation breaks down and one has to solve Eq. (24b) numerically to obtain the initial spin deviations. Like a stationary ILSR, the moving ILSR has weak plane-wave tails in the off-central region. Figure 6(b) shows the time evolution of an ILSR with $s_{\max}=0.7$, $Ka=\pi/32$, and $A=1.0$. The maximum spin deviation is modest and the ILSR can still travel through the lattice, but it is scattered by the discreteness of the lattice and the decay into plane waves is apparent. By the time of $800T_{\mathrm{ZB}}$, about 5% of the energy has decayed into the plane-wave modes. The larger its amplitude and the faster its velocity, the more emission of plane spin-wave modes. However, the stationary mode of the same maximum spin deviation is much more stable in our simulations as shown in Fig. 4(a).

B. Collision of ILSR's

Another important aspect of the nonlinear dynamics is how localized excitations interact with each other. A fundamental property of solitons is that they pass through each other as noninteracting particles. Recent studies have shown that this is not the case for intrinsic localized modes in discrete lattices, and both energy transfer between intrinsic localized modes and collision-induced decay into plane-wave modes are observed in computer simulations.[11,34]

In the FM chains we investigate, solitonlike behavior is expected for small-amplitude ILSR's. To launch two small-amplitude ILSR's moving toward each other, two small-amplitude ILSR's obtained from Eq. (19) are placed 256 sites apart in a chain of 512 spins with periodic boundary condition. The NNN interaction parameter $A=1.0$. The parameters for the two ILSR's are left, $s_{\max}=0.2$, $Ka=-\tau/25.6$; right, $s_{\max}=0.3$, $Ka=\pi/25.6$. The collision is plotted in Fig. 7(a). Before and after collision the two modes move with uniform velocity and maintain their original shapes. More accurate integration shows that the energy transfer between them is less than 0.5% of the total energy.

When ILSR's with large spin deviation (i.e., stronger nonlinearity) are involved in a collision different behavior is observed: the interaction between them becomes more violent as the mode amplitude increases. As an example, the collision between a large amplitude stationary ILSR with a small amplitude traveling ILSR in a chain of 256 spins is shown in Fig. 7(b). Each mode maintains its own shape before the collision, they interact strongly when they meet, and both become unstable after collision. Only a fraction of the small-amplitude traveling ILSR can pass through the stationary ILSR, and it decays quickly into plane-wave modes after the collision. Meanwhile the stationary ILSR also shakes away energy from its central region after the collision though it still remains localized over our simulation interval. When both ILSR's have large amplitudes neither can survive the collision. The observation reported in Ref. 11 that the collision between intrinsic localized vibrational modes tends to favor the growth of the larger excitation is not seen in our simulations for the ferromagnetic chain with both NN and NNN interactions. One possible reason is that the frequency

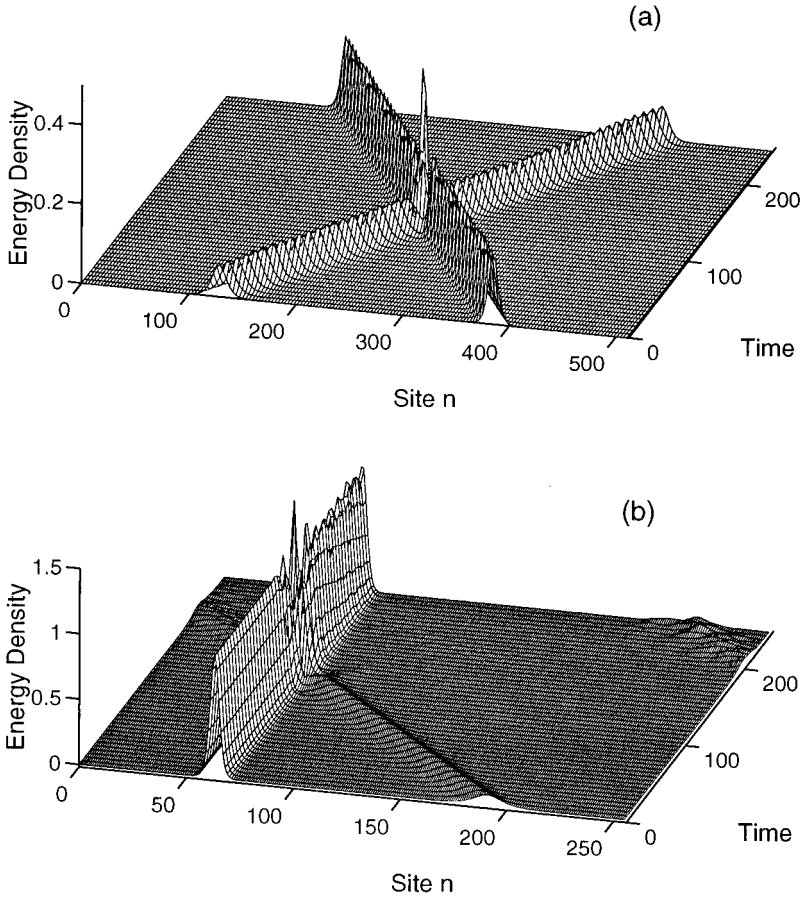

FIG. 7. Collision between two ILSR's. (a) Two traveling small-amplitude ILSR's in a chain of 512 spins with $A=1.0$. The parameters for the two ILSR's: left, $s_{max}=0.2$, $Ka=-\pi/25.6$; right, $s_{max}=0.3$, $Ka=\pi/25.6$. The two ILSR's pass through each other as noninteracting particles. The energy transfer between them is less than 0.5% of the total energy after one collision. (b) A traveling small-amplitude ILSR and a stationary large-amplitude ILSR in a chain of 256 spins with $A=1.0$. The small-amplitude ILSR are characterized by $s_{max}=0.2$, $Ka=\pi/32$, and the stationary ILSR by $s_{max}=0.7$, $Ka=0$. Both modes are unstable after the collision.

of an ILSR is in the linear spectrum and thus it strongly interacts with plane-wave modes, and the NNN coupling tends to spread the energy.

V. CONCLUSIONS

For isotropic exchange coupling and no anisotropy terms in the 1D Hamiltonian we have found that when the strength of NNN exchange interaction relative to the NN interaction exceeds a specific threshold value then ILSR's of both odd and even parity may appear in the small-amplitude plane spin-wave spectrum. A common feature of both ILSR's is that the spin deviations do not disappear with increasing distance from the center. For small spin deviations, the frequency of an ILSR lies close to the Brillouin-zone boundary frequency of the linear spin-wave band. Our numerical simulations demonstrate that the lifetime of an ILSR depends on the mode parity, the maximum spin deviation, and the relative strength of the NNN interaction to the NN one. MD simulations demonstrate that the modulation instability of the extended band-edge mode provides a possible mechanism for the creation of ILSR excitations from extended modes. In the small-amplitude continuum approximation for a given maximum spin deviation, the traveling ILSR and stationary ILSR have the same envelope shape; its width is inversely proportional to the maximum spin deviation and increases with increasing NNN coupling strength. The properties of translating ILSR depend on the size of the spin deviation. If the maximum spin deviation is modest the ILSR can travel through the lattice, but it is scattered by the discreteness of the lattice and decays into plane spin waves over sufficient distances: the larger its amplitude, or the faster its velocity, the larger the emission of plane-wave modes. For colliding ILSR's solitonlike behavior is found for small spin deviations but for large amplitudes neither can survive the collision.

ACKNOWLEDGMENTS

This work was supported in part by NSF-DMR-9631298, and ARO-DAAH04-96-1-0029. Some of this research was conducted using the resources of the Cornell Theory Center, which receives major funding from the National Science Foundation and New York State, with additional support from other members of the center's Corporate Partnership Program.

*Permanent address: Institute of Spectroscopy of Russian Academy of Science, Troitsk, Moscow 142092.

[1] G. B. Whitham, *Linear and Nonlinear Waves* (Wiley, New York, 1974).

[2] A. Newell, *Solitons in Mathematics and Physics* (SIAM, Philadelphia, 1985).

[3] H.-J. Mikeska and M. Steiner, Adv. Phys. **40**, 191 (1991).

[4] M. Toda, *Theory of Nonlinear Lattices* (Springer-Verlag, New York, 1989).

[5] M. J. Ablowitz and J. F. Ladik, J. Math. Phys. (N.Y.) **17**, 1011 (1976).

[6] A. S. Dolgov, Sov. Phys. Solid State **28**, 907 (1986).

[7] A. J. Sievers and S. Takeno, Phys. Rev. Lett. **61**, 970 (1988).
[8] V. M. Burlakov, S. A. Kiselev, and V. N. Pyrkov, Phys. Rev. B **42**, 4921 (1990).
[9] J. B. Page, Phys. Rev. B **41**, 7835 (1990).
[10] K. W. Sandusky, J. B. Page, and K. E. Schmidt, Phys. Rev. B **46**, 6161 (1992).
[11] T. Dauxois and M. Peyrard, Phys. Rev. Lett. **70**, 3935 (1993).
[12] D. Cai, A. R. Bishop, and N. Gronbech-Jensen, Phys. Rev. Lett. **72**, 591 (1994).
[13] S. A. Kiselev, S. R. Bickham, and A. J. Sievers, Phys. Rev. B **50**, 9135 (1994).
[14] S. A. Kiselev, S. R. Bickham, and A. J. Sievers, Comments Condens. Matter Phys. **17**, 135 (1995).
[15] S. Aubry (unpublished).
[16] S. Flach and C. R. Willis (unpublished).
[17] O. Bang and M. Peryard, Phys. Rev. E **53**, 4143 (1996).
[18] S. Takeno and M. Peryard, Physica D **92**, 140 (1996).
[19] S. Takeno and K. Kawasaki, Phys. Rev. B **45**, R5083 (1992).
[20] R. F. Wallis, D. L. Mills, and A. D. Boardman, Phys. Rev. B **52**, R3828 (1995).
[21] S. Rakhmanova and D. L. Mills, Phys. Rev. B **54**, 9225 (1996).
[22] R. Lai, S. A. Kiselev, and A. J. Sievers, Phys. Rev. B **54**, R12 665 (1996).
[23] R. Lai and A. J. Sievers, Phys. Rev. B **55**, R11 937 (1997).
[24] S. Takeno and A. J. Sievers, Solid State Commun. **67**, 1023 (1988).
[25] W. H. Press *et al.*, *Numerical Recipes in Fortran: The Art of Scientific Computing* (Cambridge University Press, New York, 1992).
[26] J. P. Boyd, Nonlinearity **3**, 177 (1990).
[27] J. L. Martin and S. Aubry, Nonlinearity **9**, 1501 (1996).
[28] A. Tsurui, Prog. Theor. Phys. **48**, 1196 (1972).
[29] Y. S. Kivshar and M. Peryard, Phys. Rev. A **46**, 3198 (1992).
[30] U.S. Kivshar and M. Salerno, Phys. Rev. E **49**, 3543 (1994).
[31] N. Flytzanis, S. Pnevmatikos, and M. Remoissenet, J. Phys. C **18**, 4603 (1985).
[32] K. W. Sandusky and J. B. Page, Phys. Rev. B **50**, 866 (1994).
[33] J. M. Bilbault and P. Marquie, Phys. Rev. B **53**, 5403 (1996).
[34] V. M. Burlakov and S. A. Kiselev, Sov. Phys. JETP **72**, 854 (1991).
[35] T. Rossler and J. B. Page, Phys. Rev. Lett. **78**, 1287 (1997).